Interaction Notes

Note 359

February 1979

The Circumferential Current Distribution on an Infinite Circular Cylinder Above a Ground Plane

D. R. Wilton
University of Mississippi
University, Mississippi 38677

and

K. R. Umashankar
Air Force Weapons Laboratory
Kirtland AFB, New Mexico 87117

ABSTRACT

The distribution of current on an infinite circular cylinder parallel to a ground plane and illuminated by a plane wave is obtained through the solution of an integral equation. Only that component of current flowing parallel to the axis of the cylinder and produced by a plane wave whose electric vector is parallel to and incident normal to the cylinder axis is considered. Current distributions are presented for various combinations of cylinder radii, distance above the ground, and angle of incidence.

ACKNOWLEDGMENT

The authors thank Dr. Carl E. Baum of the Air Force Weapons Laboratory for helpful suggestions and discussions.

Interaction Notes

Note 359

February 1979

The Circumferential Current Distribution on an Infinite Circular Cylinder Above a Ground Plane

D. R. Wilton
University of Mississippi
University, Mississippi 38677

and

K. R. Umashankar
Air Force Weapons Laboratory
Kirtland AFB, New Mexico 87117

ABSTRACT

The distribution of current on an infinite circular cylinder parallel to a ground plane and illuminated by a plane wave is obtained through the solution of an integral equation. Only that component of current flowing parallel to the axis of the cylinder and produced by a plane wave whose electric vector is parallel to and incident normal to the cylinder axis is considered. Current distributions are presented for various combinations of cylinder radii, distance above the ground, and angle of incidence.

ACKNOWLEDGMENT

The authors thank Dr. Carl E. Baum of the Air Force Weapons Laboratory for helpful suggestions and discussions.

THE CIRCUMFERENTIAL CURRENT DISTRIBUTION ON AN INFINITE CIRCULAR CYLINDER ABOVE A GROUND PLANE

I. INTRODUCTION

In the formulation of the problem of determining the current distribution on finite cylindrical structures, it is usually necessary to assume that the cylinder is thin so that the current density around the circumference of the cylinder is uniform. When this is not the case, one must solve a coupled set of integral equations as has been done by Kao [1-3]. This method is impractical for very long cylinders, however, as one is limited by the storage capacity of the computer. Harrison [4] has shown that at least the qualitative features of the circumferential variation of the axial component of current on a cylinder in free space may be obtained quite simply by treating the infinite cylinder. He points out that for the infinite cylinder with an incident electric field polarized parallel to the axis of the cylinder, there exists no mechanism for the excitation of circumferentially directed currents, thus decoupling the set of integral equations. Furthermore, since the cylinder is infinite, the current distribution is the same at any cross-section and the integral equation becomes one-dimensional. Harrison shows that for circular cylinders in free space

it is not necessary to solve an integral equation at all, but simply solve the boundary value problem using cylindrical wavefunctions.

If the cylinder lies parallel to an infinite perfectly conducting ground as in Figure 1a, one may employ image theory and replace the ground by equivalent image currents as shown in Figure 1b. Again, to attack the problem rigorously is a formidable task for long cylinders. However, if the cylinder is of infinite extent, then for the polarization shown in Figure 1 (termed TM polarization) a rather simple integral equation for the surface current density J_z can be derived.

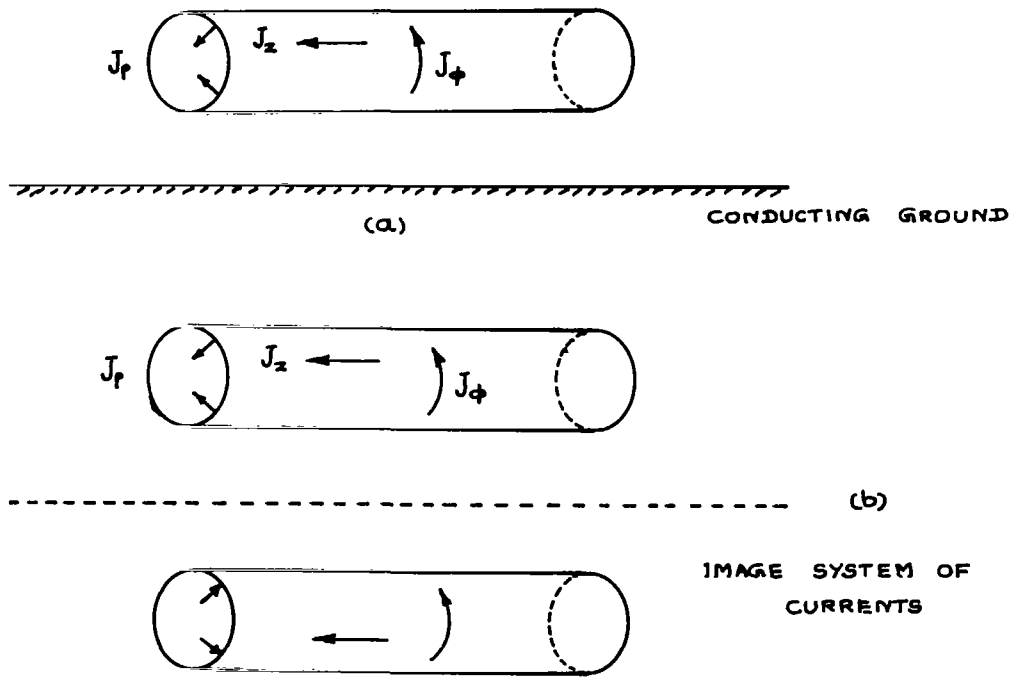

FIGURE 1. (a) FINITE LENGTH CONDUCTING CYLINDER ABOVE A GROUND PLANE (b) GROUND REPLACED BY EQUIVALENT SYSTEM OF IMAGE CURRENTS

In this report, the resulting integral equation is solved for the current distribution with a plane wave incident perpendicular to the cylinder axis. It is noted that the problem could be treated alternatively as a boundary value problem using cylindrical wavefunctions similar to the methods used by Row [5] and Olaofe [6] in the scattering by parallel cylinders. With either approach, however, one must solve a linear system of equations, but the integral equation approach has the advantage that it is also applicable to cylinders of arbitrary cross-section.

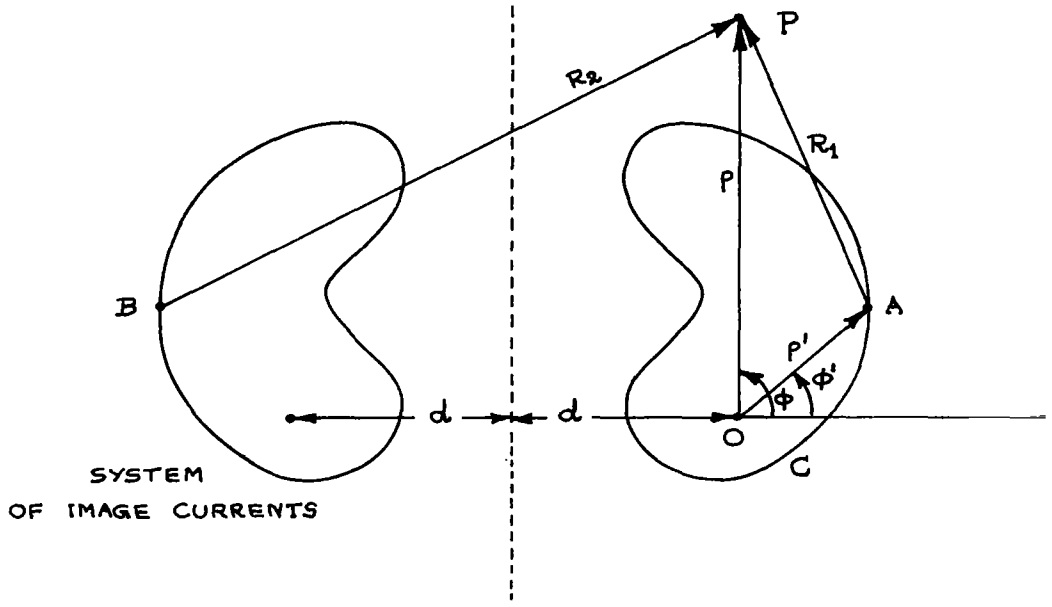

FIGURE. 2. GEOMETRY FOR THE TM SCATTERING OF AN INFINITE CYLINDER AND ITS IMAGE IN A CONDUCTING GROUND.

II. Formulation of the Integral Equation for the Current Density

Referring to Figure 2, a general observation point P in space is located in cylindrical coordinates by the vector $\bar{\rho} = (\rho,\phi)$ with respect to the origin 0 located inside the cylinder with boundary C. The cylinder lies parallel to and a distance d above the ground as indicated in the figure. By image theory, the axial current density J_z on the body at point A located by $\bar{\rho}' = (\rho',\phi')$ is the negative of the current at the corresponding image point B which is found by reflection in the ground plane. Thus, the scattered electric field at point P may be written from the surface current on the cylinder and its image as

$$E_z^s = -\frac{k\eta}{4} \int_C J_z(\bar{\rho}')[H_0^{(2)}(kR_1) - H_0^{(2)}(kR_2)]ds' \qquad (1)$$

where

$$R_1 = \sqrt{\rho^2 + \rho'^2 - 2\rho\rho' \cos(\phi-\phi')}$$

$$R_2 = \sqrt{\rho^2 + \rho'^2 + 2\rho\rho' \cos(\phi+\phi') + 4d(\rho \cos\phi + \rho' \cos\phi') + 4d^2}$$

In equation (1), k is the free-space wavenumber, $\eta \simeq 120\pi$ is the characteristic impedance of free space, and $H_0^{(2)}$ is the Hankel function of zero order, second kind ($e^{j\omega t}$ time dependence is assumed). The first term in brackets in

(1) is associated with the scattered field contribution due to current on the cylinder whereas the second term corresponds to the fields produced by the image.

Boundary conditions require that the sum of the scattered field E_z^s and the incident field E_z^i sum to zero on the surface C of the cylinder. Thus, letting point P lie on C and applying boundary conditions results in the integral equation,

$$\frac{k\eta}{4} \int_C J_z(\bar{\rho}')[H_0^{(2)}(kR_1) - H_0^{(2)}(kR_2)]\, ds' = E_z^i(\bar{\rho}),\ \bar{\rho} \text{ on } C \tag{2}$$

For a plane wave incident at an angle ϕ^i as defined in Figure 2, and including the reflection from the ground plane,

$$E_z^i(\bar{\rho}) = e^{jk\rho\cos(\phi-\phi^i)} - e^{-jk[2d\cos\phi^i + \rho\cos(\phi+\phi^i)]} \tag{3}$$

In order to solve equation (2), we first divide the contour C into N segments and denote the arc length on C from the point n = 1 by the variable s. End points of the segments are denoted by arc lengths s_n, n = 1, 2, ... , N. Borrowing from the terminology of the method of moments [7], we then expand the surface current in a set of basis functions

$$J_z \simeq \sum_{n=1}^{N} I_n T_n(s) \tag{4}$$

where

$$T_n(s) = \begin{cases} \dfrac{s-s_{n-1}}{s_n-s_{n-1}} & , \quad \text{for } s_{n-1} < s < s_n \\ \dfrac{s_{n+1}-s}{s_{n+1}-s_n} & , \quad \text{for } s_n < s < s_{n+1} \\ 0 & , \quad \text{elsewhere} \end{cases}$$

Equation (4) is a piecewise-linear approximation to the surface current distribution. Substituting (4) and (3) into (2) and requiring the resulting equation to hold only at the end points of the segments results in the linear system of equations,

$$\sum_{n=1}^{N} \ell_{mn} I_n = g_m, \quad m = 1, 2, \ldots, N \tag{5}$$

where

$$\ell_{mn} = \frac{k\eta}{4} \int_{s_{n-1}}^{s_{n+1}} T_n(s')[H_0^{(2)}(kR_{1m}) - H_0^{(2)}(kR_{2m})]ds' \tag{6}$$

$$g_m = E_z^i(\bar{\rho}_m) \tag{7}$$

and the subscript m means that all unprimed coordinates are to be evaluated at point m. Equation (5) constitutes a matrix equation for determining the coefficients I_n, which in turn give the current density according to (4).

The evaluation of the matrix elements (6) is further simplified by using a three-point approximation to the integration in (6);

$$\ell_{mn} \simeq \frac{k\eta}{4} \left\{ \frac{\Delta C_{n-\frac{1}{2}}}{2} \left[H_0^{(2)} \left(kR_{1m,n-\frac{1}{2}} \right) - H_0^{(2)} \left(kR_{2m,n-\frac{1}{2}} \right) \right] \right.$$

$$+ \Delta C_n \left[h_0^{(2)} \left(kR_{1m,n} \right) - H_0^{(2)} \left(kR_{2m,n} \right) \right]$$

$$\left. + \frac{\Delta C_{n+\frac{1}{2}}}{2} \left[H_0^{(2)} \left(kR_{1m,n+\frac{1}{2}} \right) - H_0^{(2)} \left(kR_{2m,n+\frac{1}{2}} \right) \right] \right\} , \quad m \neq n \qquad (8)$$

where the subscripts $n+\frac{1}{2}$ and $n-\frac{1}{2}$ refer to points $s_{n+\frac{1}{2}}$ and $s_{n-\frac{1}{2}}$ which are located half way between point s_n and points s_{n+1} and s_{n-1}, respectively. The second subscript on R_1 and R_2 denotes that they are to be evaluated at the location corresponding to the second subscript in the primed coordinates. We also define

$$\Delta C_n = \frac{s_{n+\frac{1}{2}} - s_{n-\frac{1}{2}}}{2} \quad .$$

Whenever $m = n$, R_{1mn} is zero and the corresponding term in (8) becomes infinite. However, the singularity in the Hankel function in (8) is integrable and a better approximation must be made. To do this, one may assume that $T_n(s')$ is constant over the segment ΔC_n in the integral (6) and use the small argument expansion of the Hankel function. Then

the term involving $R_{lm,n}$ in (8) is replaced by [7]

$$\frac{k\eta}{4} \Delta C_n \left[1 - j \frac{2}{\pi} \log\left(\frac{\gamma k \Delta C_n}{4e}\right)\right] \tag{9}$$

where $\gamma = 1.781 \ldots$ is Euler's constant. Equations (8) and (9) imply that the scatterer is modeled as a series of 2N line sources with every other source constrained to carry a current equal to the average of the adjacent line sources. At the match points where the boundary conditions are enforced, the line source at that location would give rise to infinite fields, so that for that point, the current must be "spread out" resulting in the approximation (9).

III. Numerical Results

In Figures 3-6 the surface current distribution and phase is given for a plane wave incident from an angle of 45° from the normal to the ground plane. In these cases, the values of ka used are 1.0 and 0.1 and d/a, the ratio of distance above the ground to the cylinder radius, is varied between 1.5, 3.0, and 11.2. It is noted that the variation of the incident field normal to the conducting ground is that of a standing wave while along the ground it is a traveling wave. Thus the illumination on the cylinder is stronger on the side of the cylinder away from the ground plane causing some of the asymmetry in the current distribution. However, at d/a = 11.2, the cylinder is at a peak in the

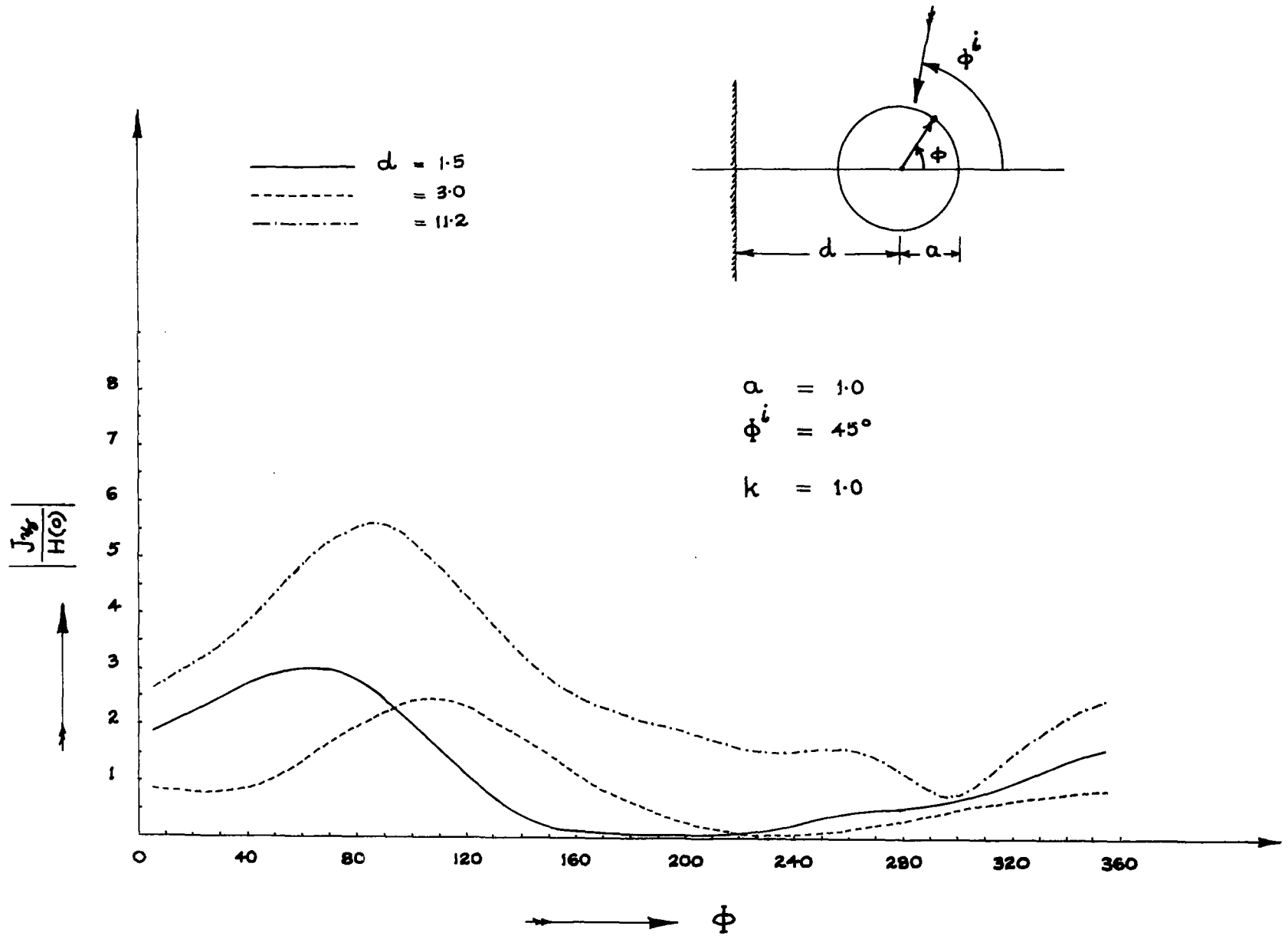

Figure 3. Magnitude of Current for ka = 1.0, ϕ^i = 45°, d/a = 1.5, 3.0, 11.2.

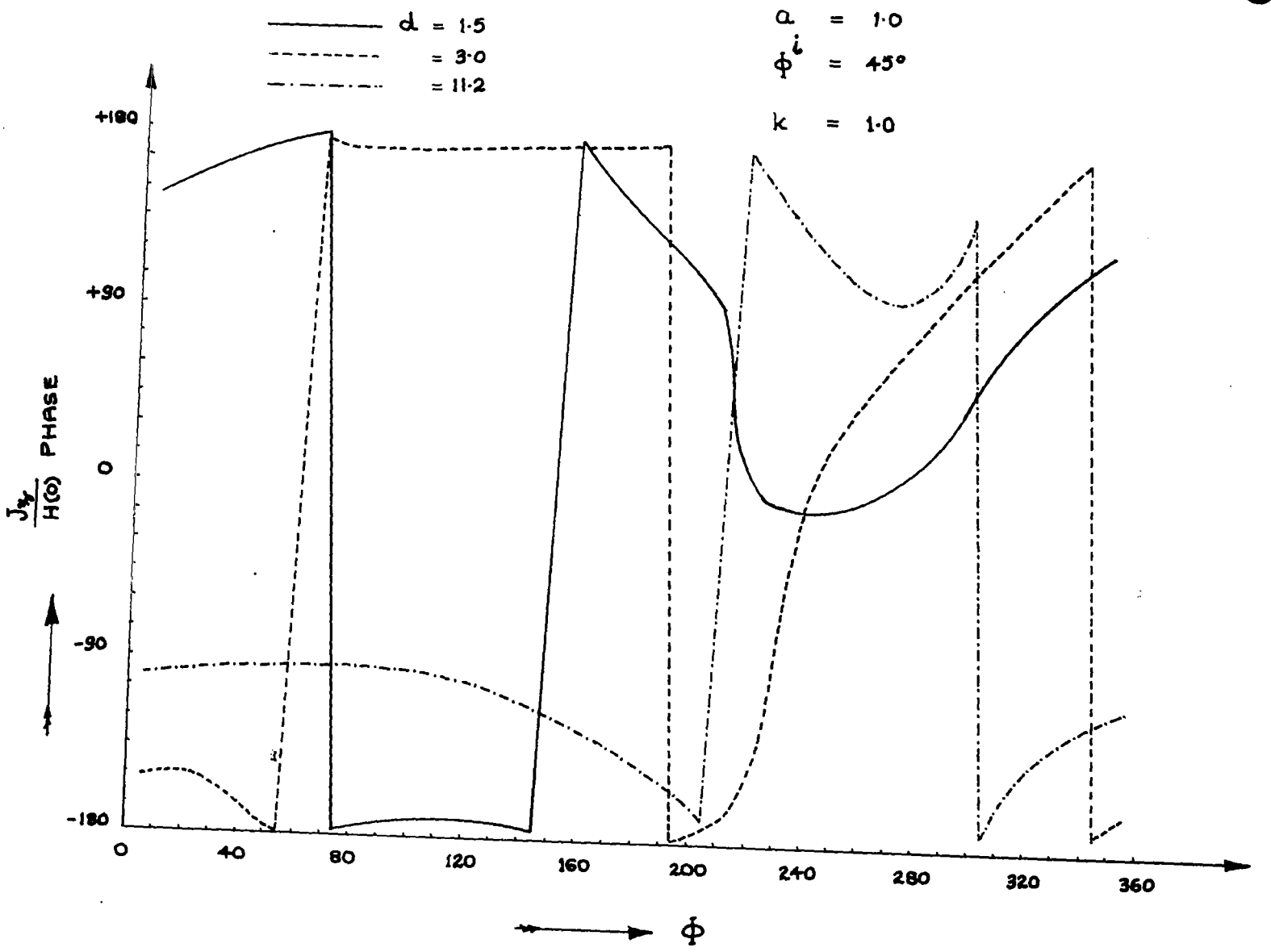

Figure 4. Phase of Current for ka = 1.0, ϕ^i = 45°, d/a = 1.5, 3.0, 11.2.

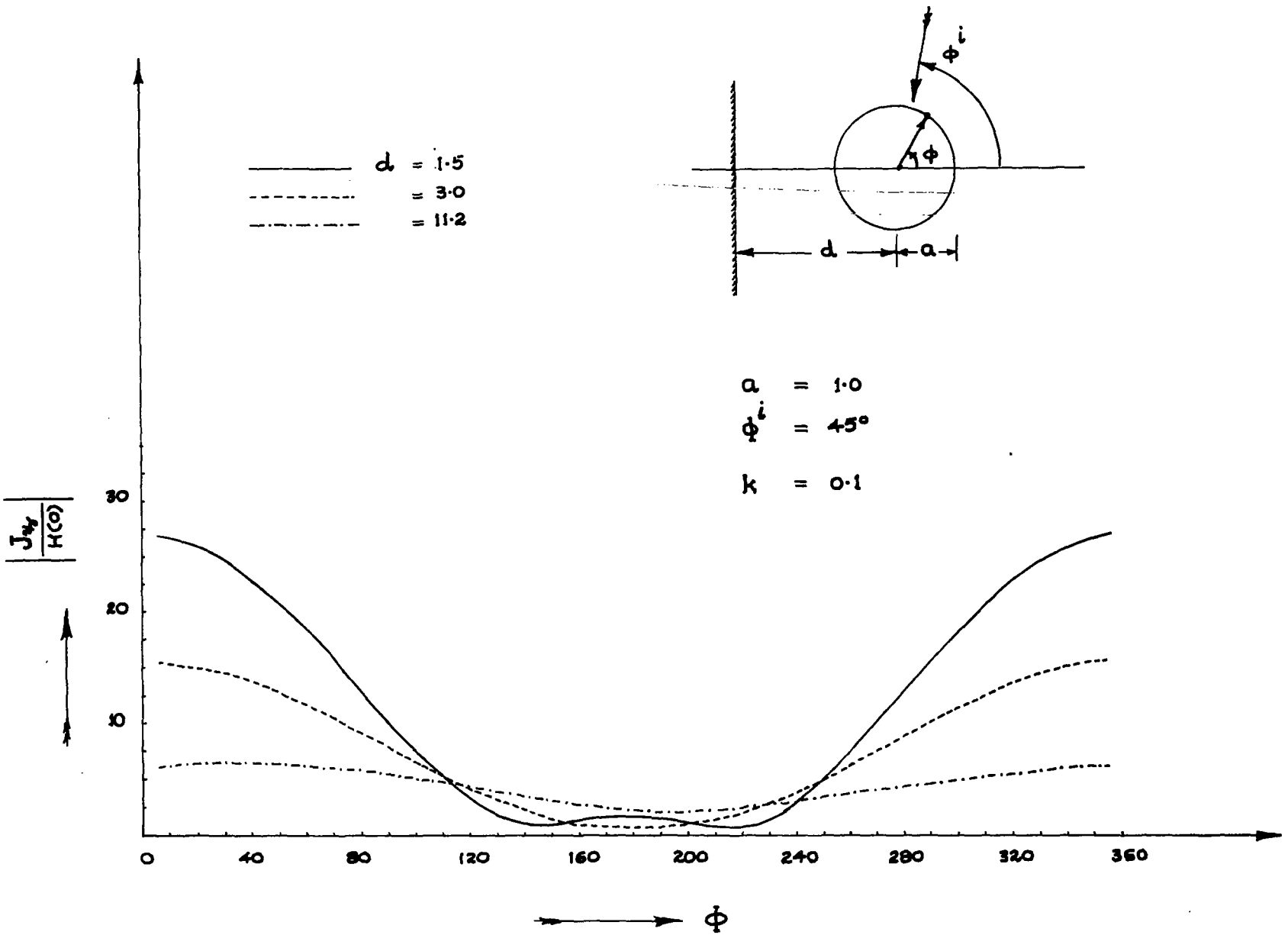

Figure 5. Magnitude of Current for ka = 0.1, ϕ^i = 45°, d/a = 1.5, 3.0, 11.2.

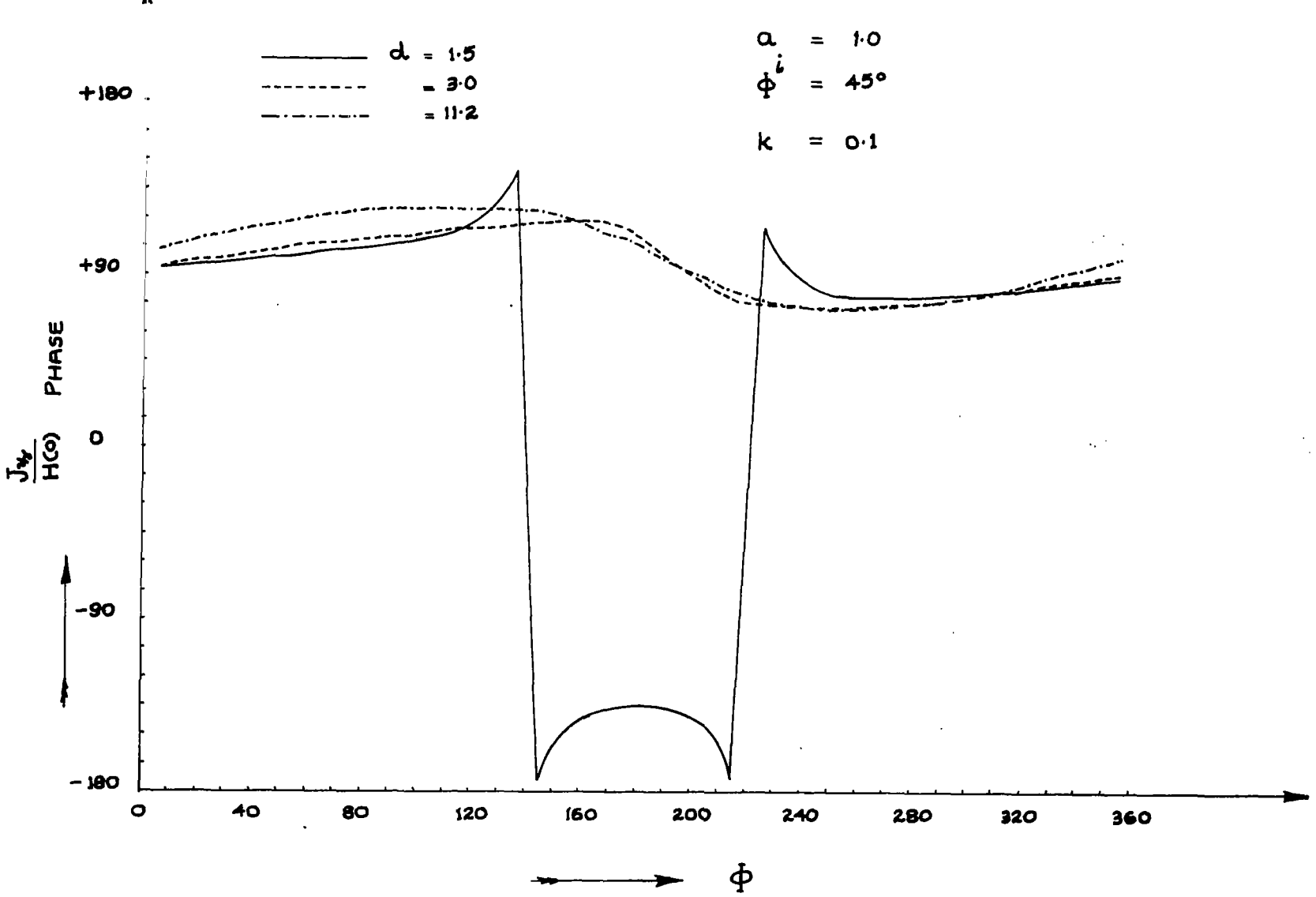

Figure 6. Phase of Current for ka = 0.1, ϕ^i = 45°, d/a = 1.5, 3.0, 11.2.

standing wave and the current distribution would be symmetric but for the coupling to the image. For small distances from the ground plane, one may determine that the forces on the charges flowing on the cylinder and its image are such as to cause the current to flow stronger on the side of the cylinder away from the ground plane. The current distributions are normalized to the incident H field at the center of the cylinder. This normalization was chosen so as to make the amplitude of the current appear less dependent on the position of the cylinder in the standing wave fields.

In Figures 7-10, the angle of incidence is 80° from the ground plane normal. For a given incident plane wave, the illumination is now much weaker since the distance to the null in the standing wave is much greater. The normalization chosen tends to make this fact less apparent in the figures, however. Again, radii of ka = 1.0 and ka = 0.1 have chosen and d/a is varied between 1.5, 2.5, 3.5, and 10.0. In Figures 11 and 12, ka = .046152 and d/a = 2.0 with 80° incidence angle is shown. These parameters roughly correspond to the fuselage of a B-52 aircraft sitting on a conducting ground pad at the lowest fuselage resonance frequency.

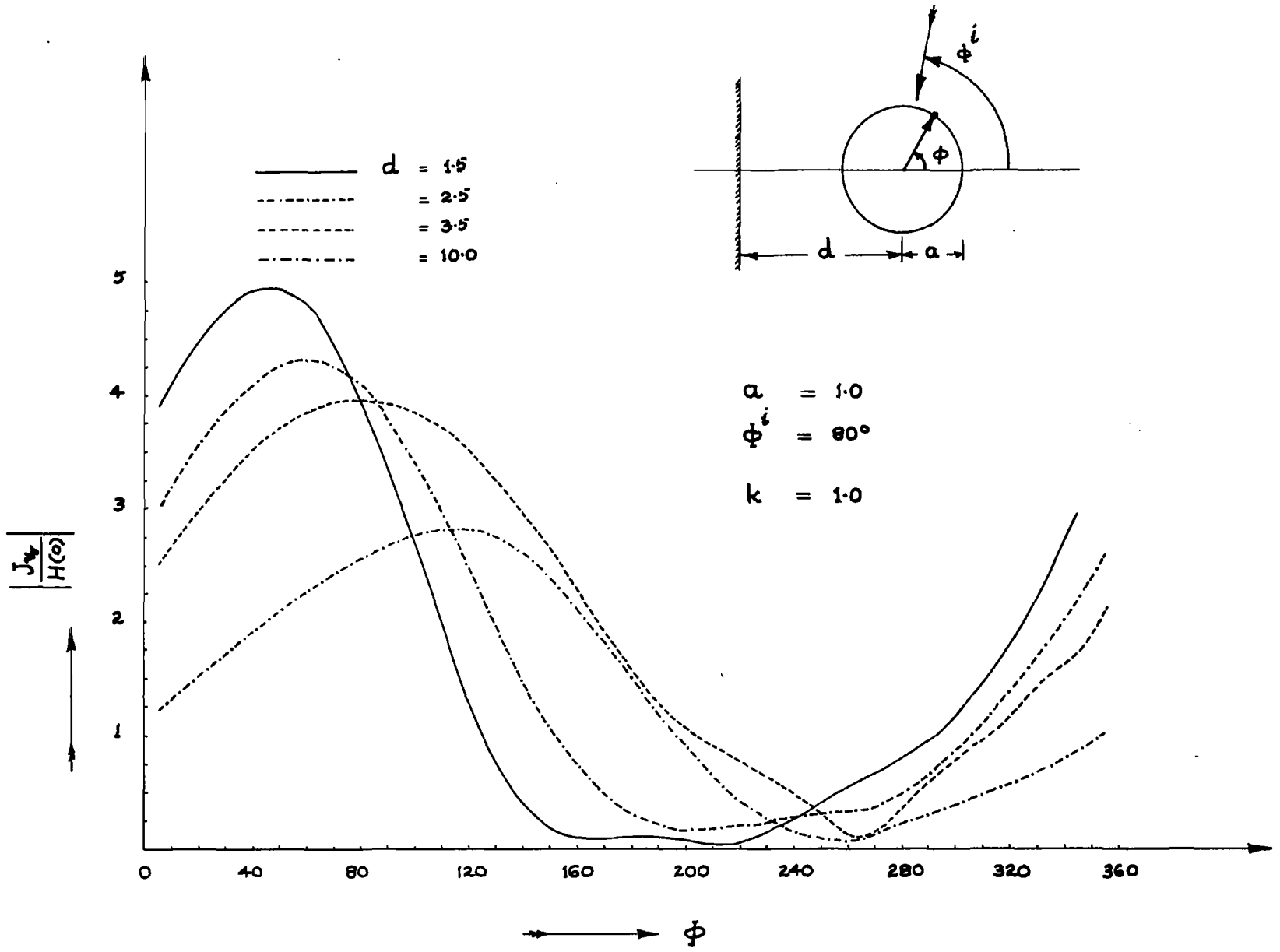

Figure 7. Magnitude of Current for ka = 1.0, ϕ^i = 80°, d/a = 1.5, 2.5, 3.5, 10.0.

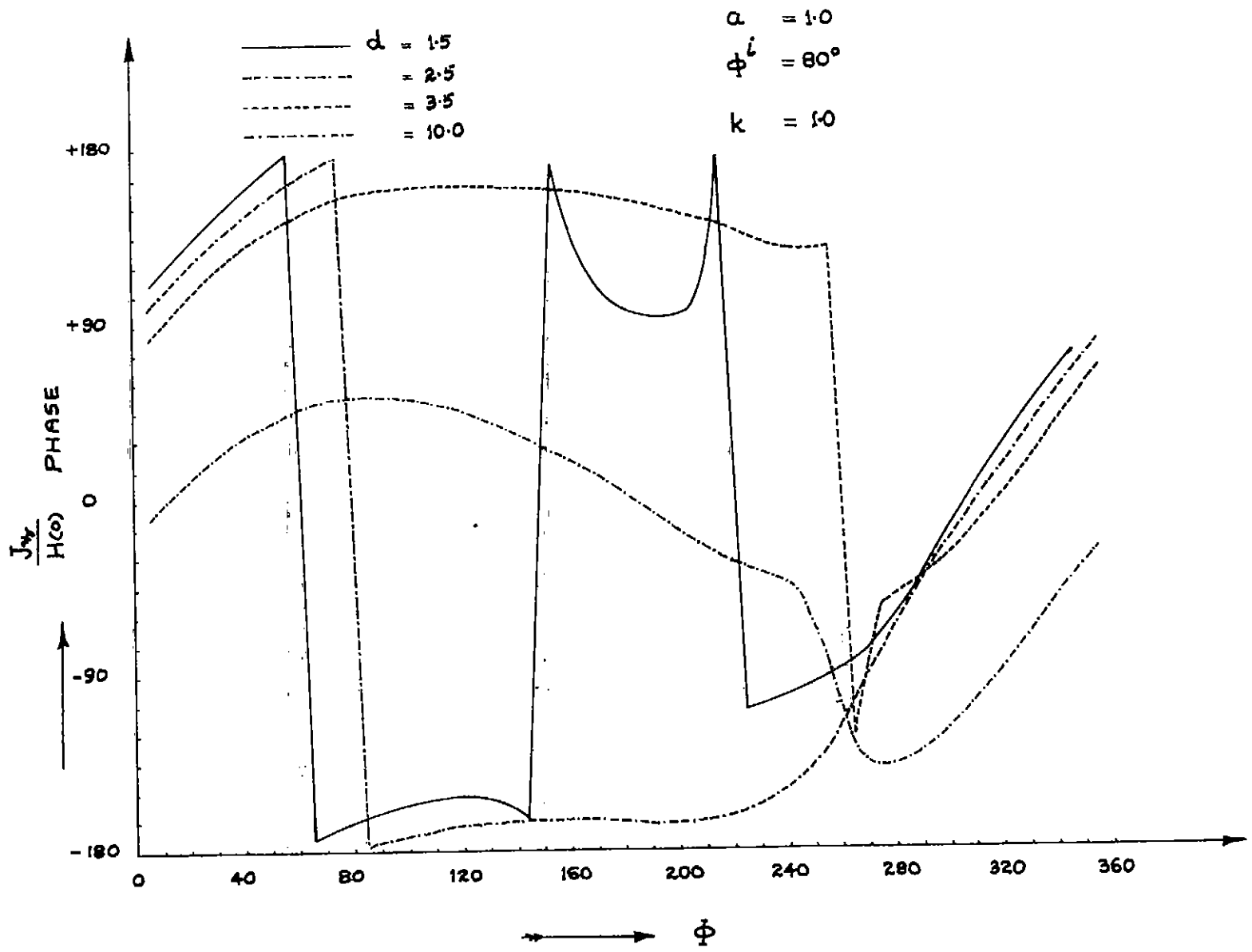

Figure 8. Phase of Current for ka = 1.0, ϕ^i 80°, d/a = 1.5, 2.5, 3.5, 10.0.

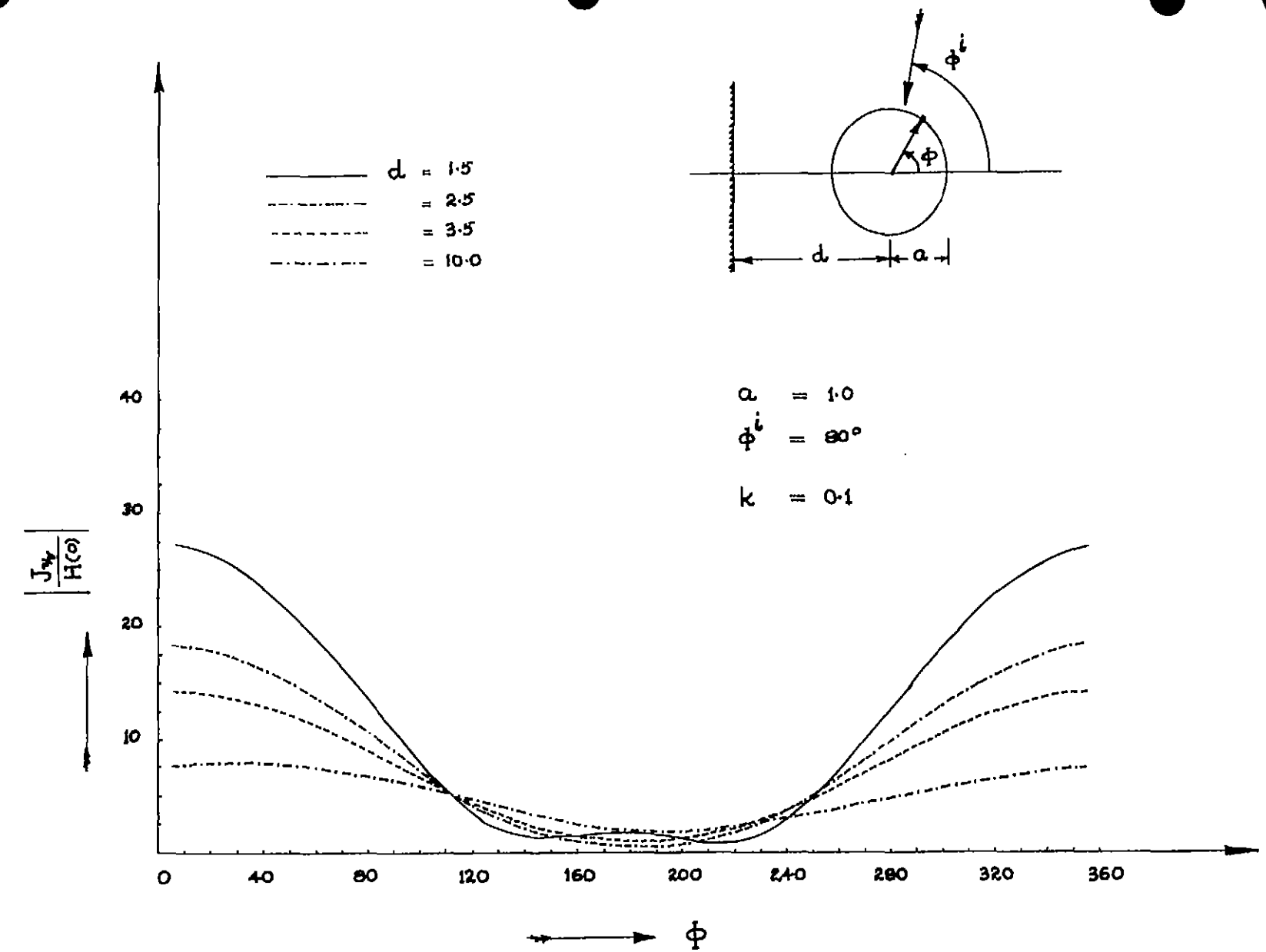

Figure 9. Magnitude of Current for ka = 0.1, ϕ^i = 80°, d/a = 1.5, 2.5, 3.5, 10.0.

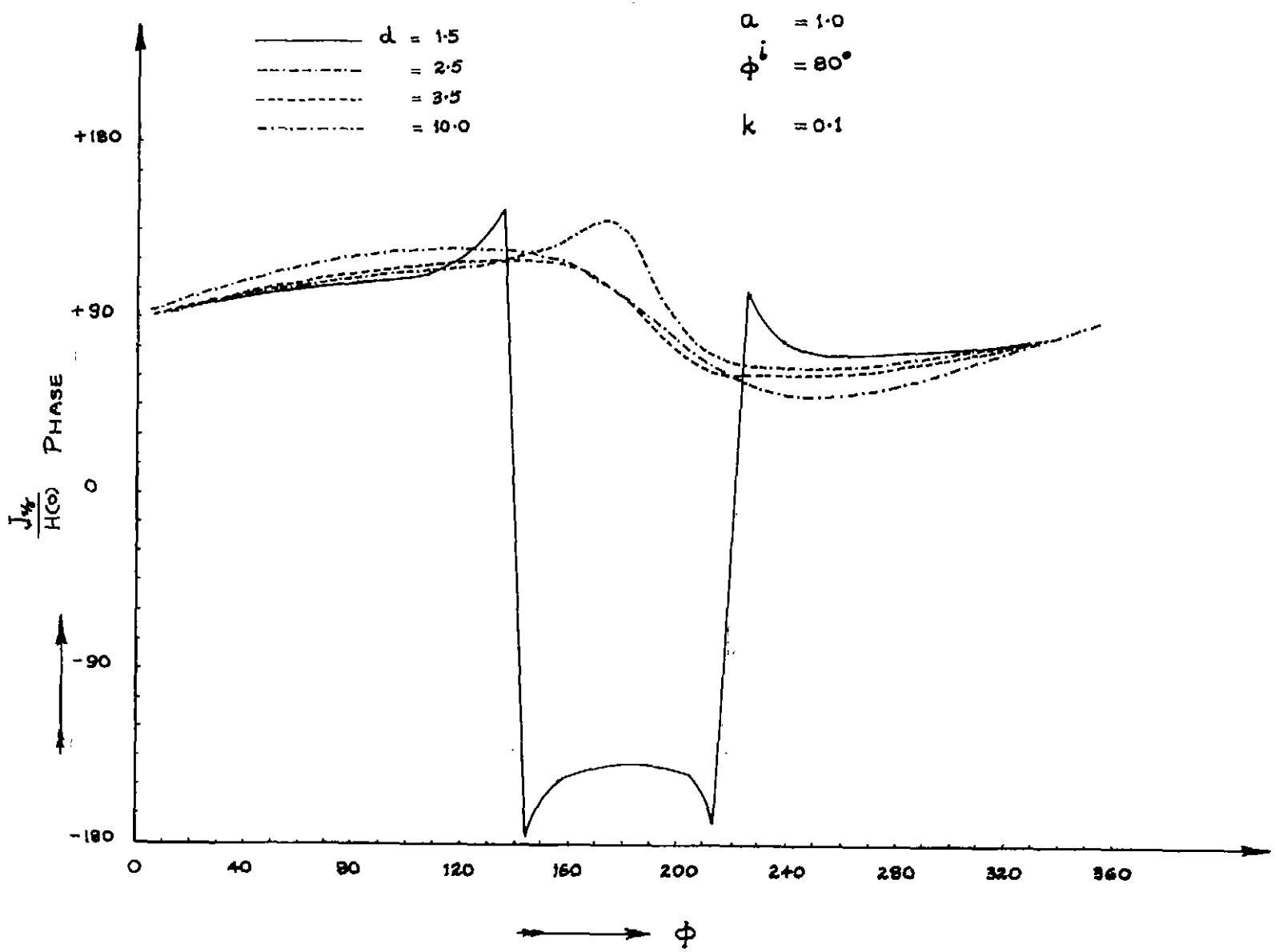

Figure 10. Phase of Current for ka = 0.1, ϕ^i = 80°, d/a = 1.5, 2.5, 3.5, 10.0.

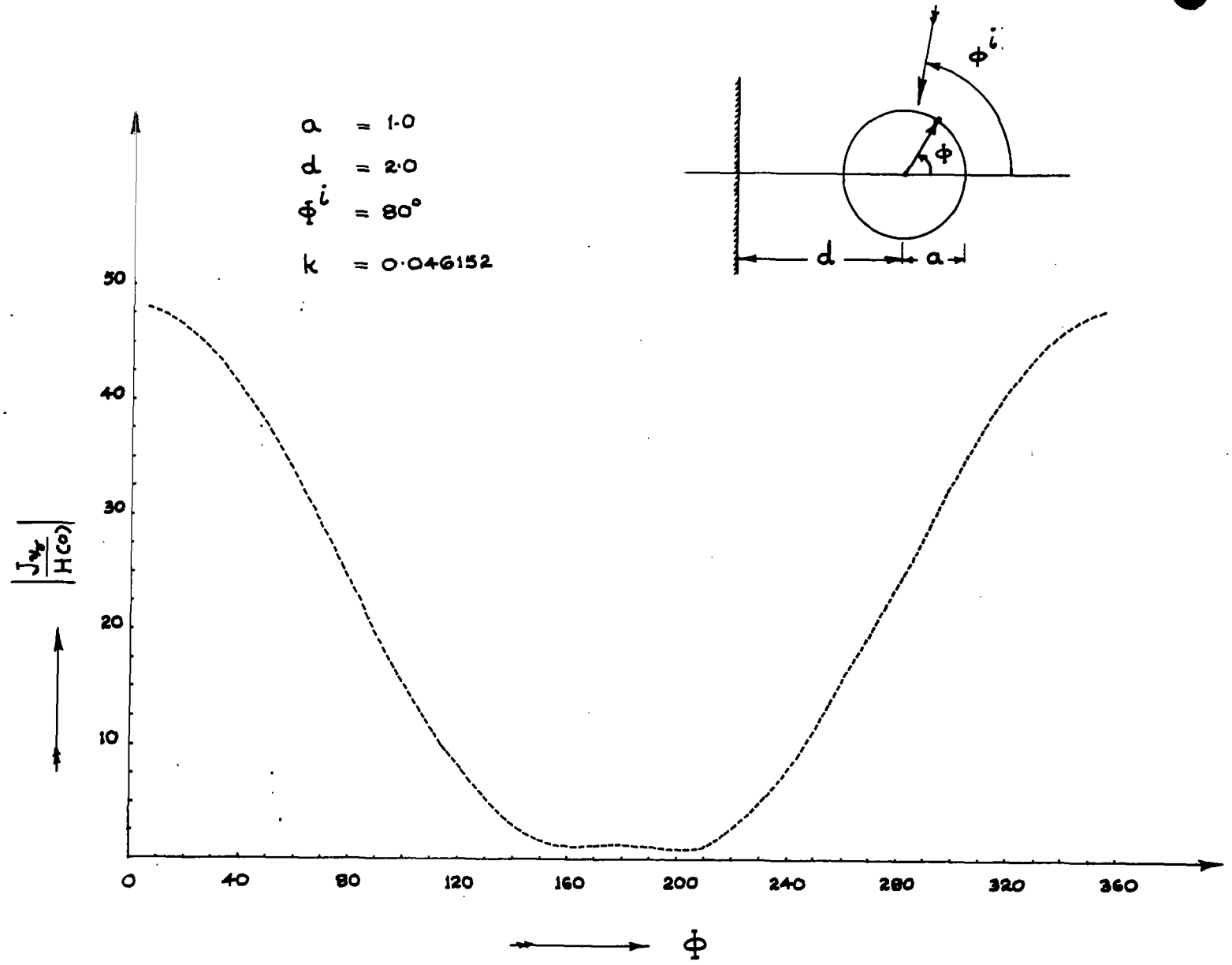

Figure 11. Magnitude of Current for ka = 0.046152, ϕ^i = 80°, d/a = 2.0.

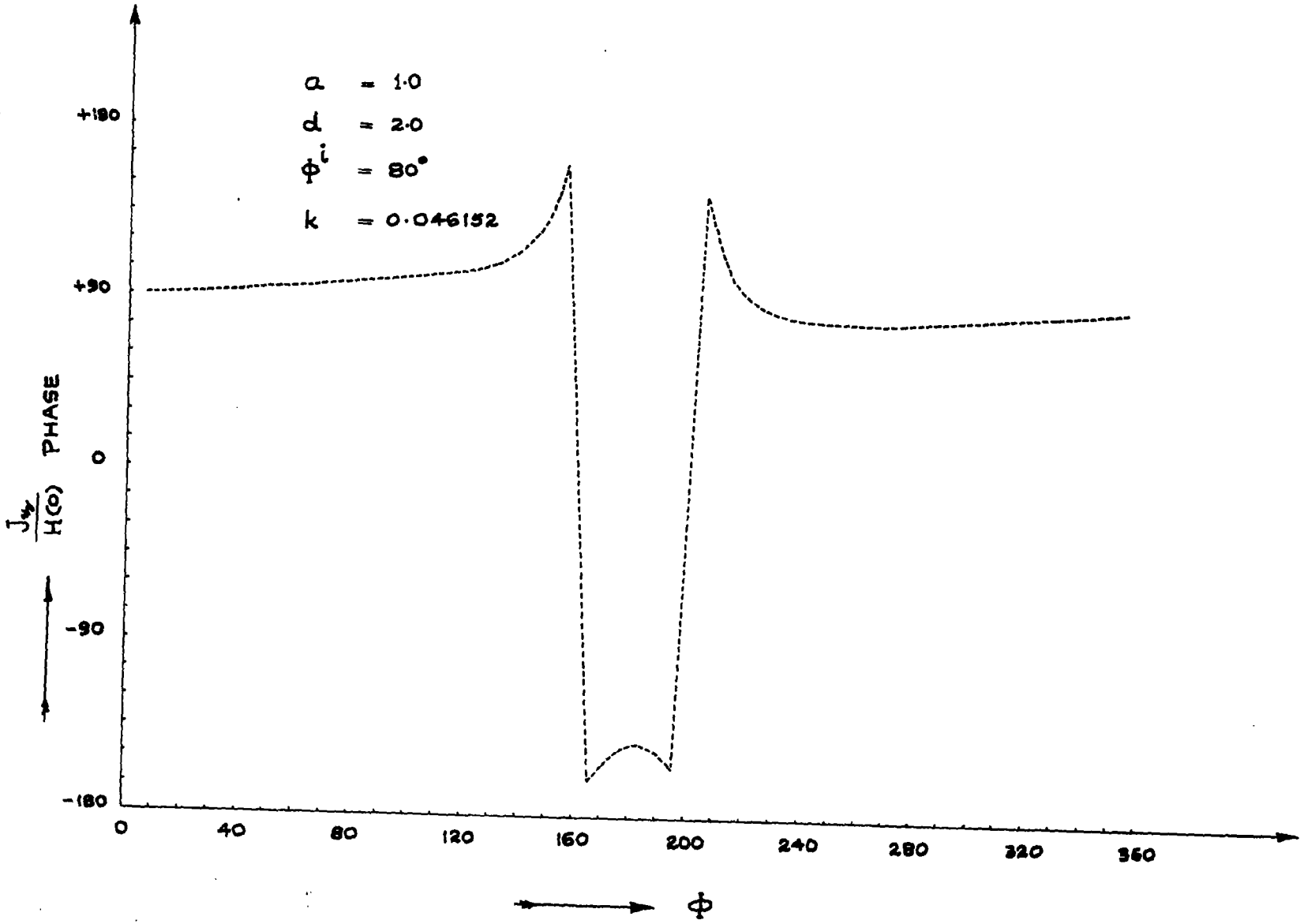

Figure 12. Phase of Current for ka = 0.046152, ϕ^i = 80°, d/a = 2.0.

In Figures 13 and 14 are shown the distribution of the current on the cylinder as a function of electrical dimension ka and fixed radio of d/a. The illuminated side has stronger currents induced and is particularly true when the cylinder is close to the ground plane. The induced current results shown in Figure 14 are split into the symmetric and the antisymmetric parts [8] with respect to $\phi = 0$ symmetry plane and are shown in Figure 15. The symmetric part of the current is obviously predominant for electrically small cylinders.

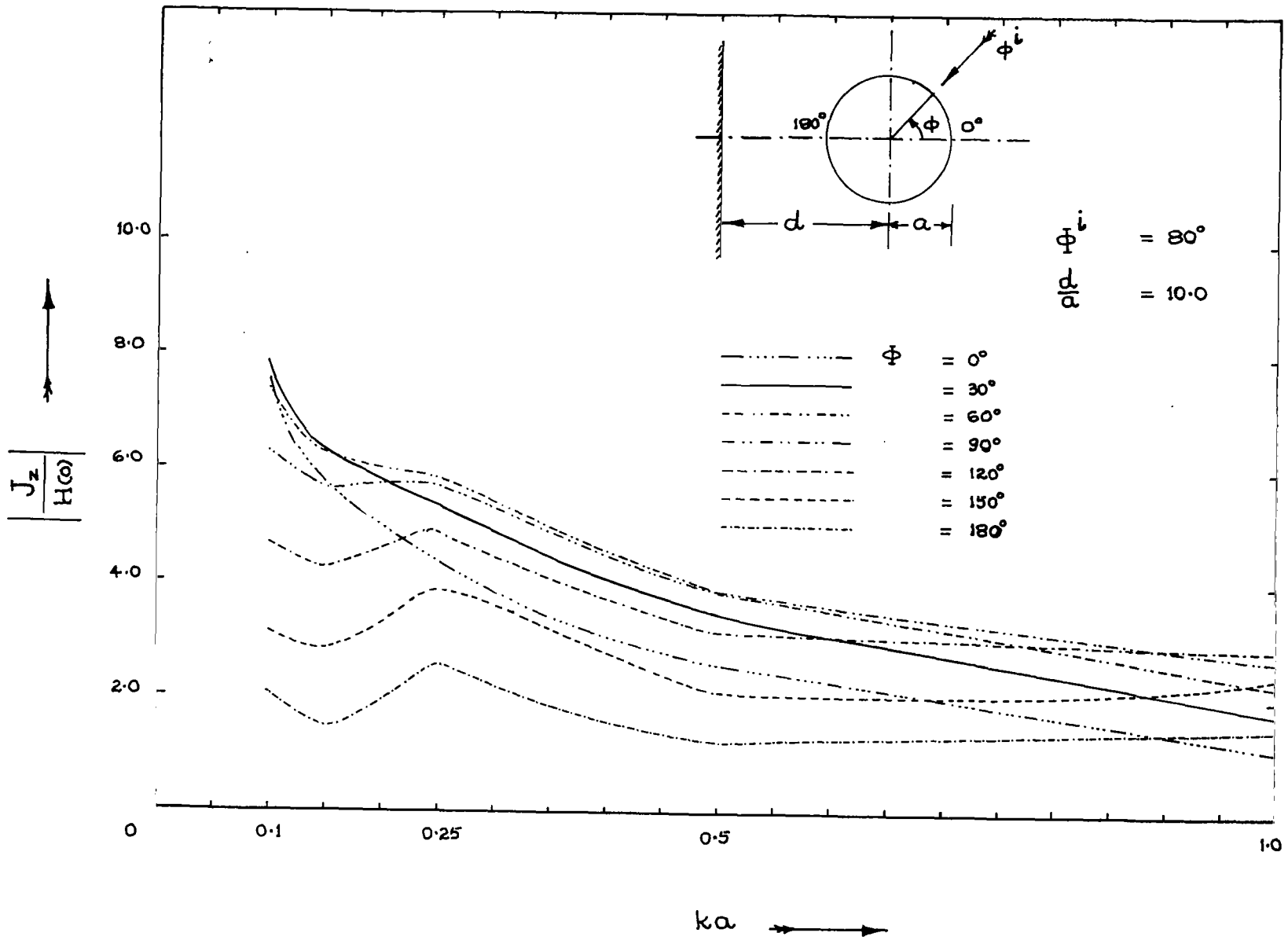

Figure 13. Magnitude of Current as a Function of ka for ϕ^i = 80°, d/a = 10.0.

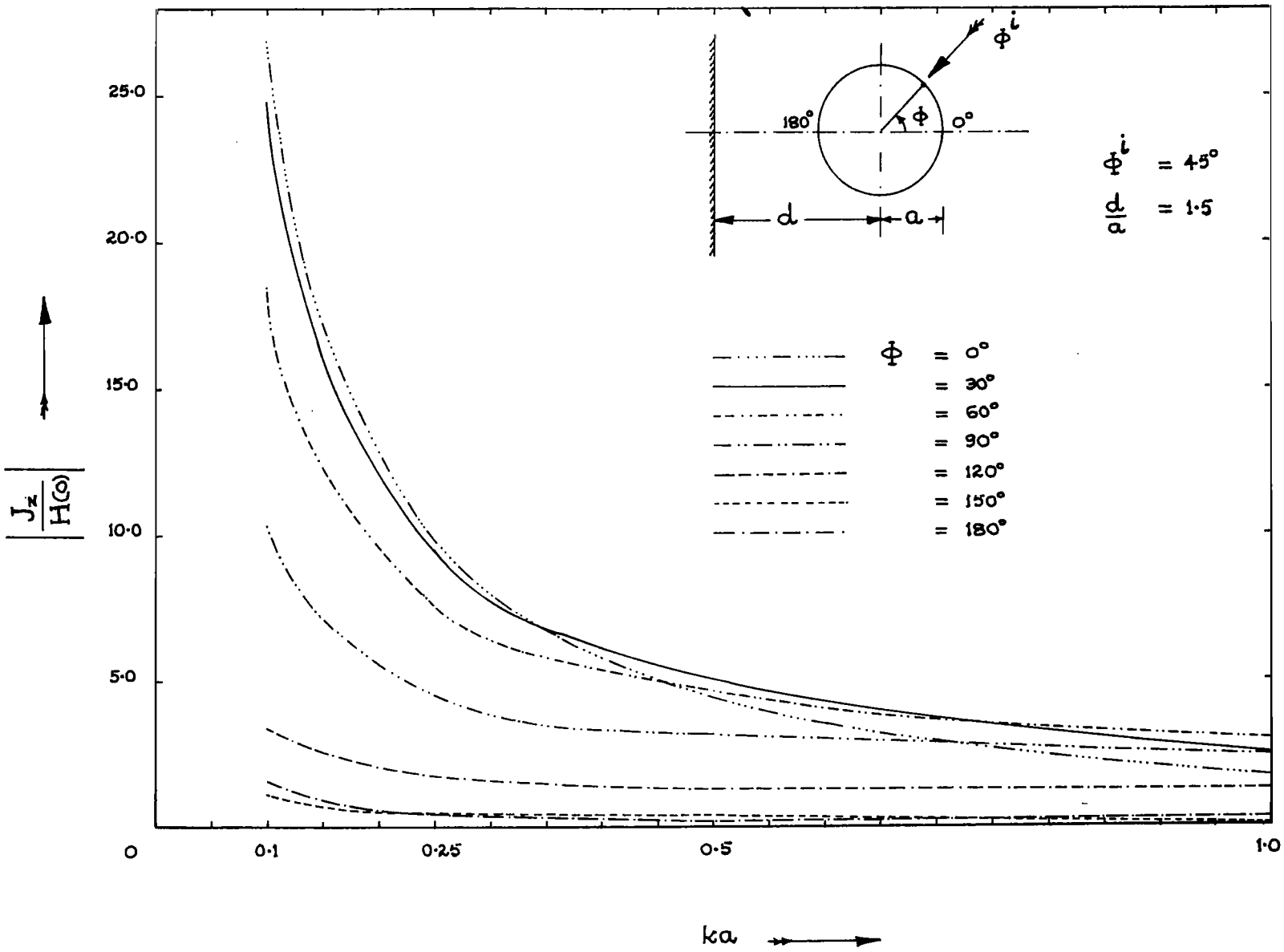

Figure 14. Magnitude of Current as a Function of ka for $\phi^i = 80°$, d/a = 10.0.

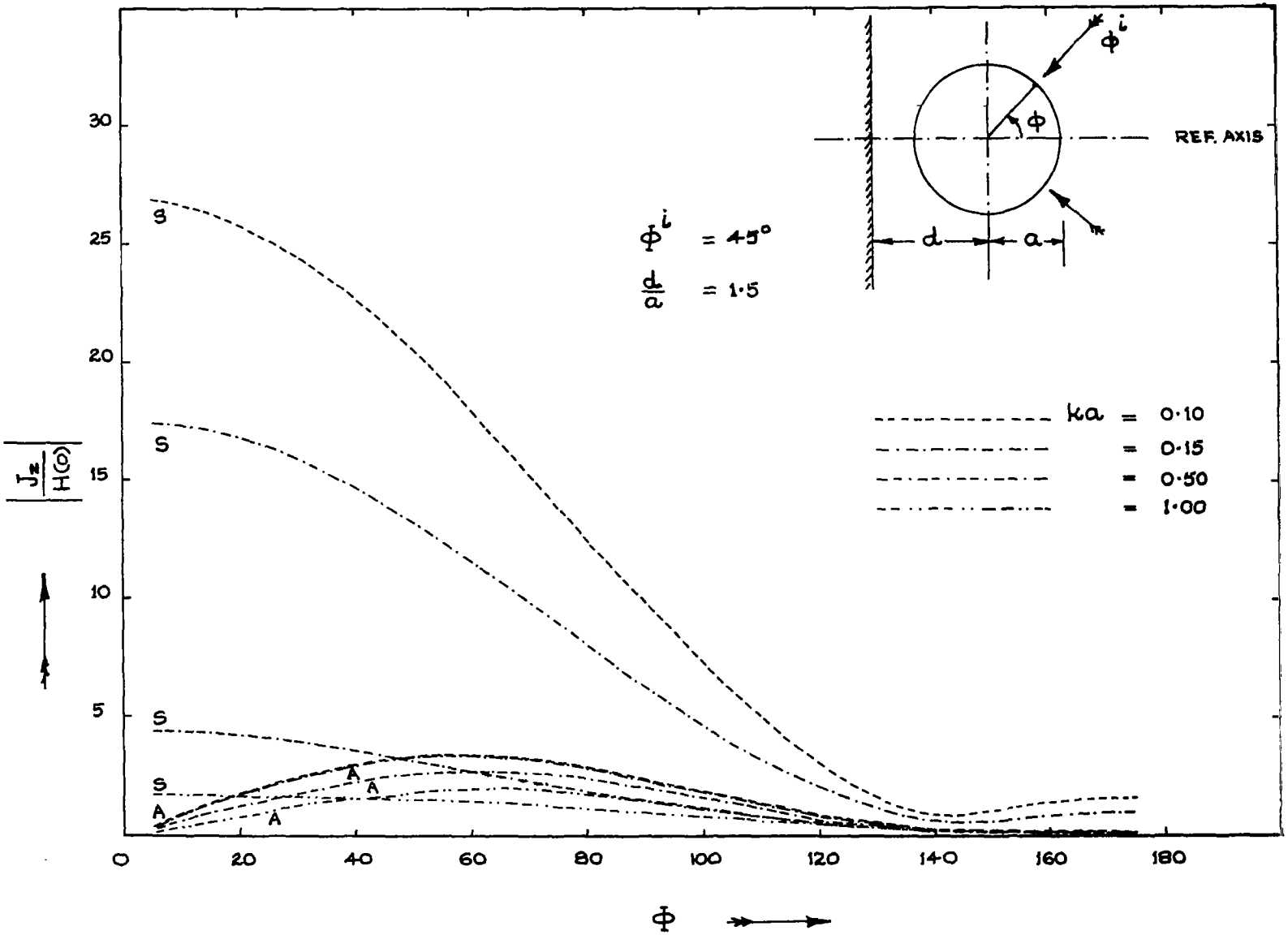

Figure 15. Magnitude of Symmetric and Antisymmetric Parts of the Current for ϕ^i = 45°, d/a = 1.5, (S = symmetric, A = Antisymmetric).

REFERENCES

[1] C. C. Kao, "Electromagnetic Scattering from a Finite Tubular Cylinder: Numerical Solutions and Data, Pt. I; Development of Theory," USAF Cambridge Research Labs., Cambridge, Mass., Rep. AF CRL-69-0535(1), Contract F 19628-68-C-0030, Dec. 1969.

[2] C. C. Kao, "Electromagnetic Scattering from a Finite Tubular Cylinder: Numerical Solutions and Data, Pt.II: Tables," USAF Cambridge Research Labs., Cambridge, Mass., Rep. AFCRL-69-0535 (2), Contract F 19628-68-C-0030, Dec. 1969.

[3] C. C. Kao, "Three-dimensional Electromagnetic Scattering from a Circular Tube of Finite Length," J. Appl. Phys., Vol. 40, Nov. 1969, pp. 4732-4740.

[4] C. W. Harrison, Jr., "Missle Circumferential Current Density for Plane Wave Electromagnetic Field Illumination," IEEE Trans. on Electromagnetic Compatibility, Vol. EMC-13, No. 2, May 1971, pp. 35-40. and also Interaction Note 60, July 1970.

[5] R. V. Row, "Electromagnetic Scattering from Two Parallel Conducting Circular Cylinders," Cruft Laboratory, Harvard University, Tech. Rep. No. 170, 1953.

[6] G. O. Olaofe, "Scattering by Two Cylinders," Radio Science, Vol. 5, No. 11, Nov. 1970, pp. 1351-1360.

[7] R. F. Harrington, Field Computation by Moment Methods, MacMillan Co., New York, 1968.

[8] C. E. Baum, "Interaction of Electromagnetic Fields with an Object Which has an Electromagnetic Symmetry Plane," Interaction Note 63, March 1971.